Evolutionary Ecology Research, 1999, **1**: 681–701

The spatial scale of pathogen dispersal: Consequences for disease dynamics and persistence

Peter H. Thrall* and Jeremy J. Burdon

Centre for Plant Biodiversity Research, CSIRO – Plant Industry, GPO Box 1600, Canberra, ACT 2601, Australia

ABSTRACT

Plant pathogens exhibit a diverse array of life histories and dispersal mechanisms. The latter suggests that, in nature, there will be a broad range of spatial scales over which hosts and pathogens interact (e.g. soil-borne pathogens to aerially dispersed rusts). Variation in the spatial scale of such interactions is likely to have consequences for disease dynamics and pathogen persistence, and therefore coevolution of host and pathogen. We investigated disease dynamics and persistence using a spatially explicit simulation model that incorporated local dispersal of host and pathogen approximating the range of spatial structures seen in nature (i.e. many small isolated populations with very local dispersal to single large populations with some sub-structuring with global dispersal). Our results show that the spatial scale of pathogen dispersal is an important factor in determining the probability of disease persistence, as well as spatial and temporal patterns of incidence. Disease persistence was highest at relatively local scales of dispersal; at higher scales, not only was disease persistence less likely, but disease also caused major reductions in the fraction of sites occupied by the host. The nature of the dynamics also varied with the spatial scale of dispersal, with temporal changes in disease presence across the metapopulation showing endemic patterns at low scales of dispersal, but epidemic patterns when pathogen dispersal was over broader scales. It has been argued that the genetic diversity of host–pathogen systems with respect to resistance and virulence will depend on the probability of encounter rates between particular host and pathogen genotypes. Our results suggest that encounter rates, and therefore genetic diversity, are also likely to be heavily influenced by the spatial scale of the interaction.

Keywords: endemic, epidemic, metapopulation, population asynchrony.

INTRODUCTION

A primary difference between the population biology of plant pathogens in agricultural contexts and natural plant communities lies in the relative importance of spatial distribution of hosts in the dynamics of disease (Burdon, 1993). Plant pathogens in natural systems are perforce patchily distributed in space because of the distribution of their host resource. This spatial structuring, coupled with the wide diversity of life-history features (e.g. severity of mortality/fecundity effects and dispersal mechanisms) encountered in pathogens as a

* Author to whom all correspondence should be addressed. e-mail: thrall@pi.csiro.au

whole, is likely to impact on pathogen persistence and patterns of disease incidence. Variation in spatial patterns of disease incidence will determine rates of encounter between host and pathogen genotypes, and will therefore influence the evolution and maintenance of variation in host resistance and pathogen virulence. Because of the 'typical' patchiness and ephemerality of disease in nature, advances in our understanding of broader evolutionary processes are most likely to come from a metapopulation approach that incorporates colonization and extinction processes (Antonovics *et al.*, 1994; Thrall and Burdon, 1997).

The classical view of metapopulations (Levins, 1969, 1970) depicts a set of populations that are randomly dispersed among an array of habitat patches, only some of which are occupied at any given time. All such local populations have similar characteristics with respect to carrying capacity, growth rates and local distributions, and consequently show equal probabilities of going extinct or of contributing migrants to other currently occupied or unoccupied sites. In turn, all empty sites have equal probabilities of being colonized. While the conceptual approach pioneered by Levins has been enormously valuable in advancing our appreciation of the importance of spatial structure for the evolutionary biology and ecology of organisms, there are many ways in which the assumptions built into his model are violated in real world systems. Indeed, as the importance of spatial variation has become more generally recognized, the metapopulation concept has been broadened to include a wider range of species dynamics, with much of the recent work exploring various extensions and departures from the Levins model (e.g. Hanski and Gilpin, 1997; Tilman and Kareiva, 1997).

The degree to which dispersal occurs at local spatial scales relative to the metapopulation as a whole is likely to be particularly important in systems in which both numerical and genetic or coevolutionary interactions occur between two or more species (Gilpin, 1975; Antonovics *et al.*, 1997). Even within single species, the scales at which colonization, extinction and gene flow occur may be quite distinct (e.g. seed *vs* pollen movement in plants: McCauley, 1994; McCauley *et al.*, 1995; Antonovics *et al.*, 1997; Thrall *et al.*, 1998). Where two or more species interact, population and genetic dynamics may potentially occur over an even broader range of spatial and temporal scales – scales that are likely to differ sharply between the component species within a single association and certainly between different combinations of species. However, relatively few studies have examined (a) the spatial and temporal dynamics of multispecies interactions, or (b) the consequences of varying the scale of these interactions (where by scale, we mean the distances over which populations interact directly; e.g. through seed movement and gene flow).

Plant host–pathogen interactions provide some of the best examples of coevolutionary metapopulation systems in which both numerical and genetic dynamics have been investigated. Although to date the number of empirical studies is relatively limited, those studies have demonstrated the importance of space in several ways. Thus, interactions between *Linum marginale* and *Melampsora lini* (Burdon and Jarosz, 1991, 1992; Jarosz and Burdon, 1991, 1992; Burdon and Thompson, 1995), *Silene* spp. and *Ustilago violacea* (Antonovics *et al.*, 1994; Thrall and Antonovics, 1995; Carlsson *et al.*, 1990), and *Filipendula ulmaria* and *Triphragmium ulmariae* (Burdon *et al.*, 1995) have all shown marked patchiness in the incidence and severity of disease from population to population. These studies have also demonstrated the importance of population size and disease status of neighbouring populations for disease occurrence (*U. violacea*, *T. ulmariae*); the lack of local correlations between the frequencies of specific virulence and resistance genes, with marked spatial fluctuations in resistance and virulence phenotypes (*M. lini*); and the highly dynamic nature

of interactions with significant extinction and recolonization rates resulting in an ephemerality of disease within individual patches (*U. violacea*, *T. ulmariae*). Theoretical models (Alexander and Antonovics, 1988; Thrall and Jarosz, 1994b), as well as field and experimental data (Antonovics *et al.*, 1994; Burdon and Jarosz, 1992; Thrall and Jarosz, 1994b), indicate that long-term pathogen persistence in these systems is unlikely to occur in any single host population, and thus can only be explained in the context of colonization/extinction processes within a metapopulation framework.

Several theoretical studies have examined the consequences of spatial structure for the population biology and evolutionary dynamics of host–pathogen interactions. Thus, Frank (1991) investigated the maintenance of genetic polymorphisms in resistance and virulence using a two-dimensional simulation approach, with random migration and homogeneous patch quality; his results showed that coevolutionary dynamics alone can maintain high levels of spatial variation in polymorphism even when migration is high and there is no environmental cause of spatial variation. Similarly, Gandon *et al.* (1996) studied the effects of different migration rates on spatial patterns of host resistance and pathogen virulence, finding that the degree of local adaptation depended on the scale of pathogen migration relative to the host. Thrall and Antonovics (1995) and Antonovics *et al.* (1997) have also studied the ecological and evolutionary dynamics of vector-transmitted plant diseases using a spatially explicit simulation approach with local dispersal and realistic distributions of environmental variation. However, in none of these studies have the consequences of varying the scale of host–pathogen interactions been investigated using explicitly spatial models.

In an earlier paper, we argued that interactions between host and pathogen life-history features are likely to have important consequences for several aspects of disease ecology and evolution in nature (Thrall and Burdon, 1997). In particular, we predicted that shifts in the relative scale of host and pathogen dispersal would influence the evolution and maintenance of genetic polymorphisms in resistance and virulence, and also have dynamical consequences for spatial and temporal patterns of pathogen persistence and prevalence. In the present study, we develop a spatially explicit simulation model to investigate the dynamical consequences of one particular pathogen life-history feature, namely the spatial scale of pathogen dispersal. We examine several aspects of disease dynamics, including local and regional persistence, and spatial and temporal patterns of disease prevalence and severity. In addition, we characterize the disease dynamics as a function of the scale of pathogen dispersal (degree to which dynamics are oscillatory, degree of synchronicity among populations).

THE MODEL

Our aim is to explore the consequences of the interaction between migration rate and the relative spatial scales of dispersal for the dynamics and persistence of host–pathogen associations. In the simulations presented below, we do not attempt to model precisely any particular disease system, but rather develop a more heuristic model that incorporates some general biology of many plant host–pathogen interactions. However, because we also wish to explore the consequences of variation in dispersal for within- and among-population dynamics, we parameterize the model using biologically realistic values derived from natural host–pathogen systems where space has been shown to play an important role in the observed patterns [in particular, the *Linum marginale–Melampsora lini* (Burdon and Jarosz,

1991, 1992; Jarosz and Burdon, 1991, 1992) and *Silene alba–Ustilago violacea* (Alexander and Antonovics, 1988; Antonovics *et al.*, 1994; Thrall and Jarosz, 1994a,b; Thrall and Antonovics, 1995; Alexander *et al.*, 1996) interactions]. For convenience, a list of model parameters and definitions is provided in the Appendix.

Although the focus of the present study is on ecological rather than evolutionary dynamics (in particular, on disease persistence and spatial patterns of disease severity and prevalence), we incorporate a minimal amount of genetic variation in the model by assuming two haploid hosts and two pathogen types (which reproduce asexually), where each pathogen is virulent on a different host type and avirulent on the other (see Frank, 1991, for a similar model). We adopt this resistance/virulence structure, not to investigate genetic dynamics *per se*, but rather as a useful indicator of the degree of among-population synchronicity (the degree to which frequencies of host and pathogen genotypes covary across patches). In the simulation results reported here, we assume that the dynamics within each patch are deterministic, whereas the dispersal and extinction/colonization phases are stochastic.

Within-population dynamics

The focus of this study is on aerially dispersed pathogens where plants can vary in the degree to which they are infected (i.e. disease severity, which, in the case of localized rusts, can be defined as the number of pustules per plant or the percentage of tissue that is infected), where multiple cycles of pathogen reproduction may occur within a season, and where the pathogens may be dispersed over broad spatial scales relative to their hosts (e.g. rusts). Note that this differs markedly from systemic plant diseases such as floral smuts (e.g. *Ustilago violacea* on members of the Caryophyllaceae; Thrall *et al.*, 1993).

If X_t, Y_t and P_t are the numbers of healthy hosts, infected hosts, and total pustules in the host population respectively at time t, then, assuming no within-season host mortality, we can write the equations for changes in disease levels following a single cycle of infection during the growing season [where $X_{t,u}$ = the number of healthy hosts after u infection cycles ($u = 1, \ldots, k$)] as:

$$X_{t,1} = X_t \, e^{-\beta P_t} \tag{1}$$

$$Y_{t,1} = Y_t + X_t(1 - e^{-\beta P_t}) \tag{2}$$

$$P_{t,1} = P_t(1 - \mu_{PS} + \gamma) + X_t(1 - e^{-\beta P_t}) \tag{3}$$

where we assume that the probability of infection is dependent on the total density of pustules present in the population (for brevity, we present only the equations for a single host and pathogen). The number of new pustules per existing pustule is given by γ, μ_{PS} is the within-season death rate for pustules, and β is the disease transmission parameter (= a measure of transmission efficiency). Similarly, after two infection cycles,

$$X_{t,2} = X_{t,1} \, e^{-\beta P_{t,1}} \tag{4}$$

$$Y_{t,2} = Y_{t,1} + X_{t,1}(1 - e^{-\beta P_{t,1}}) \tag{5}$$

$$P_{t,2} = P_{t,1}(1 - \mu_{PS} + \gamma) + X_{t,1}(1 - e^{-\beta P_{t,1}}) \tag{6}$$

Thus, the equations describing across-year changes in the numbers of healthy and infected hosts (assuming no effects of infection on host fecundity), and the number of pustules, can be written as (assuming k infection cycles per growing season):

$$X_{t+1} = b(X_t + Y_t) + X_{t,k}(1 - \mu_X) + \varepsilon Y_{t,k} \tag{7}$$

$$Y_{t+1} = Y_{t,k}(1 - \mu_Y)(1 - \varepsilon) \tag{8}$$

$$P_{t+1} = P_{t,k}(1 - \mu_Y)(1 - \mu_{PW})(1 - \varepsilon) \tag{9}$$

where ε is the rate at which infected hosts recover, μ_X and μ_Y are the mortality rates for healthy and infected hosts respectively, and μ_{PW} is the over-winter death rate for pustules. The parameter b is the per-capita host birth rate, and is assumed to be density-dependent as follows:

$$b = \frac{b_0}{1 + \zeta N_t} \tag{10}$$

where N_t is the total host population density at time t ($= X_t + Y_t$), b_0 is the maximum per-capita birth rate (at $N_t = 0$) and ζ represents the strength of density-dependence.

Long-term field data on *L. marginale–M. lini* indicates that the mortality rate of infected plants is strongly dependent on the per-plant density of pustules (disease severity). In the simulation, we therefore assume a logistic function for mortality:

$$\mu_Y = \frac{\mu_0}{1 + a\lambda^{-P_t/Y_t}} \tag{11}$$

where μ_0 is the maximum death rate of infected plants, λ determines the rate at which mortality increases with disease severity and $a = \mu_0/\mu_X - 1$.

As noted, equations (7)–(9) assume that infection does not affect host birth rate, but only over-winter survival. Thus, the scenario we are describing is one in which reproduction occurs independently of infection, but where there is differential over-winter survival of healthy and infected hosts following k infection cycles during the growing season. This is perhaps most representative of situations where host reproduction occurs relatively early in the growing season before pathogen numbers are high (e.g. *L. marginale–M. lini*).

Among-population processes

For the metapopulation simulations, we assumed a two-dimensional array of patches with absorbing boundaries, where each patch was assigned a carrying capacity at random from a log-normal distribution (mean = 100, range = 2–1000); these were reassigned at random for each simulation run. In the simulation, we solve for ζ in each population based on the carrying capacity that it has been assigned, using equation (10).

In each time interval, a fraction of the spores (m_P) and seeds (m_X) produced in each patch were dispersed according to a Weibull probability distribution where the probability of landing in a site that is i units from the source is given by:

$$W(i) = e^{-(i/a)^{\theta}} - e^{-((i+1)/a)^{\theta}} \tag{12}$$

and the parameters α and Θ control the scale and shape of the dispersal curve respectively (Martz and Waller, 1982). In the simulation, Θ was fixed at 1, and α and the maximum spore dispersal distance were varied simultaneously such that the total probability of migrating spores falling within the specified distance was approximately unity ($\alpha = 0.25$, 0.5, 1.25, 2.0, 3.0, 5.0, 8.0; the maximum distance dispersed = 2, 5, 10, 15, 20, 30, 45 population units respectively). This scheme allowed us to examine the effects of dispersal in situations ranging from single isolated populations with little or no among-population connectedness (dispersal distance = 0, 2) to those in which the simulation essentially behaved as a single large population with some degree of substructuring (dispersal distance = 30, 45). In the remainder of the paper, we refer to pathogen dispersal distances of 0–5 as 'low', of 10–20 as 'intermediate' and of 30–45 as 'high'. Two levels of pathogen migration were investigated: $m_P = 0.05$ and 0.2. The total probability of infection occurring within a patch was therefore a function of the spores migrating in from other diseased patches (discounted by the fraction of resistant hosts in the focal patch) plus the average level of disease severity (i.e. number of pustules per plant) within the patch.

With respect to host dispersal, we assumed one of two dispersal distances (5, 15), where the number of resident seeds in a patch (following reproduction) was discounted by the fraction of seeds dispersed out ($m_X = 0.05$ for all simulations). Whether or not seeds that dispersed out of patches successfully colonized was determined by a fixed probability of establishment.

Within each host generation, 5–8 infection cycles took place – the exact number being determined at random, but biased to produce a frequency distribution of 1 : 2 : 2 : 1 (i.e. years with 5 or 8 infection cycles were less common than years with 6 or 7 cycles). This pattern fits with data from populations of a variety of aerially dispersed pathogens. In contrast, the models of Frank (1991, 1993) and Gandon *et al.* (1996) assumed host and pathogen generation times of the same length, with no possibility of within-season epidemic build-up.

Following within-population reproduction, dispersal and establishment of new host and pathogen populations, over-winter death of adults and recovery of infected plants was allowed to occur. At the beginning of each time interval, prior to the within-population dynamics phase, a probability of extinction was calculated for each occupied patch as a hyperbolic function of population size (see Thrall and Antonovics, 1995).

In the results reported here, each simulation was allowed to run for a maximum of 300 generations (= years). After 150 generations, spatial and temporal patterns (e.g. fraction of occupied sites, average population sizes, degree to which dynamics were oscillatory) had generally become stable, and data were then collected and averaged over the remaining 150 generations. For each set of initial conditions, 100 random runs were done. Data on colonization and extinction rates were taken at the beginning of each growing season after over-winter mortality, recovery and disturbance; data on the fraction of occupied sites, the fraction of sites with disease present, disease prevalence within populations, and disease severity (pustules per plant) were taken at the fifth disease cycle within each growing season. In many host–pathogen systems, this would, on average, approximate to a midpoint in the seasonal build-up of disease. Only runs in which both pathogen types persisted for the entire 300 generations were used to generate overall averages, or investigate spatial and temporal patterns. For comparative purposes, we iterated equations (7)–(9) for a single population and no migration (i.e. no spatial structure), using the same parameter values as for the simulation, but assuming strictly deterministic dynamics.

Parameter estimation from field data

Disease transmission

Estimates of β were derived from data on disease spread in natural populations of *Linum marginale* and *Melampsora lini* (J.J. Burdon, unpublished data). Under the assumption of non-linear density-dependent disease transmission, the probability of infection [$= 1 - \exp(-\beta P_t)$; see equations (1)–(3)] was calculated from the number of newly infected plants observed at a census point during the growing season versus the total density of disease pustules in the population at the previous census point; these data were fitted using non-linear regression (β was estimated as 0.0006). This value was used in all simulation runs.

Spore/pustule production

The number of spores produced by a single pustule is dependent not only on the density of pustules on a leaf, but also on the rust species in question. For the purposes of the simulation, we used the results of Leonard (1969) for *Puccinia graminis* as a general guide to choosing a value of 20,000 spores per pustule. Rough estimates of per-capita pustule production were obtained by reworking raw data from an experiment involving the development of *M. lini* infections from single pustules (Burdon and Elmqvist, 1996). In the simulation, we assumed that the maximum possible number of pustules per plant was 300. This number was based on estimates of the severity of disease (percent area covered by pustules) suffered by *L. marginale* plants naturally infected with *M. lini*. These values were converted to numbers of pustules with allowance being made for plant size (= numbers of stems).

Mortality/recovery rates

Mortality rates for healthy and infected plants – and, in the latter case, the relationship between mortality and the degree of disease severity – were all estimated from a sequence of 10 years of epidemiological and demographic data for the *L. marginale–M. lini* interaction. The rate of recovery of infected plants to healthy susceptible plants was estimated from the same data set. The average mortality rate for healthy plants (μ_X) = 0.15. The maximum mortality rate for infected plants (μ_0) = 0.95, the dependence of the infected mortality rate on disease severity (λ) = 1.02, and the recovery rate (ε) = 0.85. These values were used in all simulation runs (see equation 11).

Temporal and spatial patterns of disease

We examined several aspects of temporal dynamics in relation to the spatial scale of pathogen dispersal. First, we measured the relationship between the amplitude of global fluctuations in the frequencies of host and pathogen genotypes, and the fraction of diseased populations. This was done by estimating the statistical variance around the mean values of each of 20 random runs (where mean host and pathogen frequencies were obtained by summing across all occupied sites in the metapopulation, and averaging). Second, for each run, we measured the number of times host and pathogen genotype frequencies fluctuated across their mean values; this provided some measure of the degree to which dynamics were oscillatory. Third, we examined the statistical correlation between host and pathogen genotype frequencies across the metapopulation as a whole for each generation within a run. Although we only show data for the case when host dispersal was at the higher scale (= 15),

and the pathogen migration rate was 0.2, the results were qualitatively similar for the other cases investigated.

We were also interested in spatial patterns of disease incidence and severity; for five random runs representing each of the initial conditions (2 levels of host dispersal × 7 levels of pathogen dispersal × 2 levels of pathogen migration rate), we collected information on disease prevalence, disease severity and the frequency of associated host and pathogen genotypes at the 300th generation (as well as the spatial location of each extant population). These data were analysed using the program GS+/386 (Gamma Design Software, 1994); Moran's *I* was calculated to evaluate the degree of spatial structure for each of the different scenarios.

SIMULATION RESULTS

Disease prevalence and persistence

Probability of disease persistence

In all cases, the scale of pathogen dispersal had a complex non-linear effect on the probability of disease persistence. When among-population pathogen dispersal was excluded (dispersal distance = 0, small isolated populations), regional persistence did not occur. However, as the scale of pathogen dispersal increased, the probability of disease persistence across the metapopulation as a whole rose rapidly to a maximum, before falling, and then rising slowly once more (Fig. 1). Interestingly, the probability of persistence was lowest when pathogen dispersal was at intermediate ranges. Overall, the pathogen migration rate had a very substantial effect (compare Figs 1A,B); regardless of the scale of host dispersal, increasing the migration rate generally caused a reduction in the likelihood of pathogen persistence. In contrast, for any given pathogen migration rate, persistence was substantially increased when host dispersal was at the larger spatial scale (= 15; Fig. 1, dotted lines). When host dispersal was at the smaller scale (= 5; Fig. 1, solid lines), pathogen persistence rarely occurred at intermediate scales of spore dispersal. The same general patterns were observed with respect to the average persistence time of disease in the metapopulation.

Fraction of sites occupied

Pathogen migration rate had no effect on the fraction of sites occupied by the host (after reaching stable dynamics at the metapopulation level). Overall, increasing the spatial scale of pathogen dispersal led to dramatic decreases in the fraction of occupied sites, particularly for low to intermediate dispersal distances (Fig. 2A). The shape of the interaction between occupancy and spatial scale was very similar for different host dispersal distances, although the more local scale of host dispersal resulted in significantly higher occupancy for intermediate pathogen dispersal distances; pathogen persistence was also lowest over this range of dispersal distances.

Fraction of populations with disease present

Regardless of migration rate, the fraction of diseased populations was always greater when host dispersal was greater (Fig. 2B). With respect to pathogen dispersal, the most noticeable

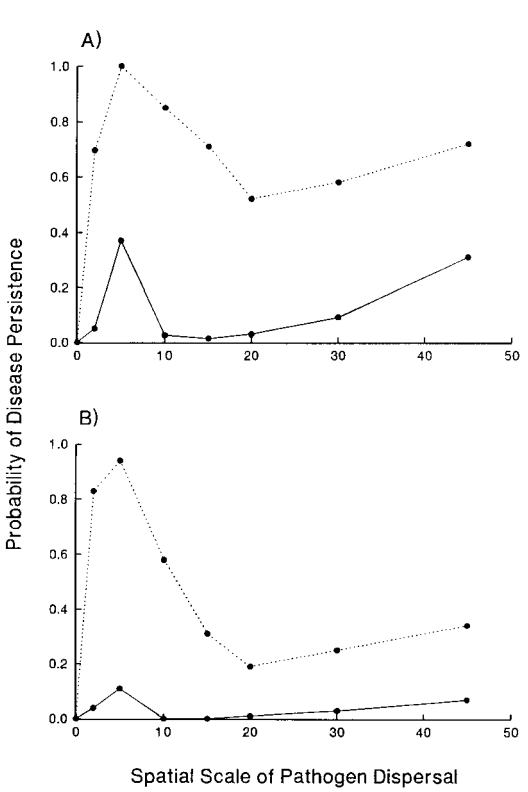

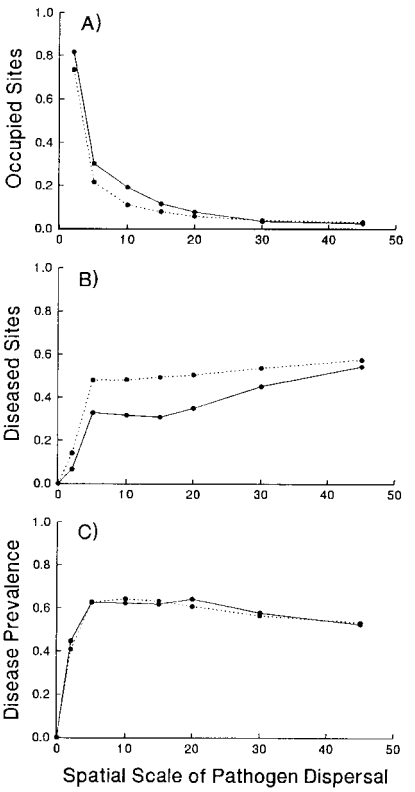

Fig. 1. (Left) Probability of disease persistence (defined as the fraction of simulation runs that persisted for at least 300 generations) as a function of the maximum spatial scale of pathogen dispersal. Each point represents the mean of 100 random runs, except where sample sizes were small (pathogen dispersal = 10–20, host dispersal = 5) due to low persistence. In these cases, an extra 500 runs were performed to generate sufficient data for the graphs. Solid lines are for host dispersal distance = 5; dotted lines are for host dispersal distance = 15. (A) Pathogen migration rate = 0.05; (B) pathogen migration rate = 0.2. Other parameter values were $b_0 = 1.25$, $\beta = 0.0006$ (for both pathogens), $\gamma = 3.0$, $\varepsilon = 0.85$, $\mu_X = 0.15$, $\mu_0 = 0.95$, $\mu_{PS} = 0.5$, $\mu_{PW} = 0.97$.

Fig. 2. (Right) Disease patterns across the metapopulation as a function of the spatial scale of pathogen dispersal. Data shown are for when the pathogen migration rate = 0.05 (essentially the same pattern was seen when the pathogen migration rate was fixed at 0.2). (A) Fraction of sites that were occupied (out of 3600 possible); (B) fraction of occupied sites with disease present; (C) average prevalence of infection within diseased populations. In all graphs, solid lines are for when host dispersal distance = 5 and dotted lines are for host dispersal distance = 15. All other parameters are the same as for Fig. 1.

effect occurred at low dispersal scales, where the fraction of populations with disease present increased sharply. Above this point, there was a very slow increase in disease as dispersal rate increased. In general, the fraction of diseased populations was higher for the lower pathogen migration rate.

Disease prevalence

Neither host dispersal distance nor pathogen migration had any discernible effect on average disease prevalence (fraction of infected individuals in a population). Similar to the relationship observed for the fraction of populations with disease present, there was a sharp increase in average disease prevalence for low pathogen dispersal scales (Fig. 2C). However, at higher scales of pathogen dispersal, disease prevalence showed a slow but steady decline. This was in contrast to the slow increase observed with respect to the fraction of diseased populations.

Metapopulation growth rates

Generally, both host and pathogen colonization and extinction rates were unaffected by the pathogen migration rate. With respect to the host, the relation between metapopulation growth rate (= colonization – extinction) and the spatial scale of pathogen dispersal was similar for both scales of host dispersal, showing a continuing smooth decline (positive for low pathogen dispersal and negative for large; Fig. 3A). The rate of decline in host metapopulation growth rate was greater when host dispersal was over shorter distances.

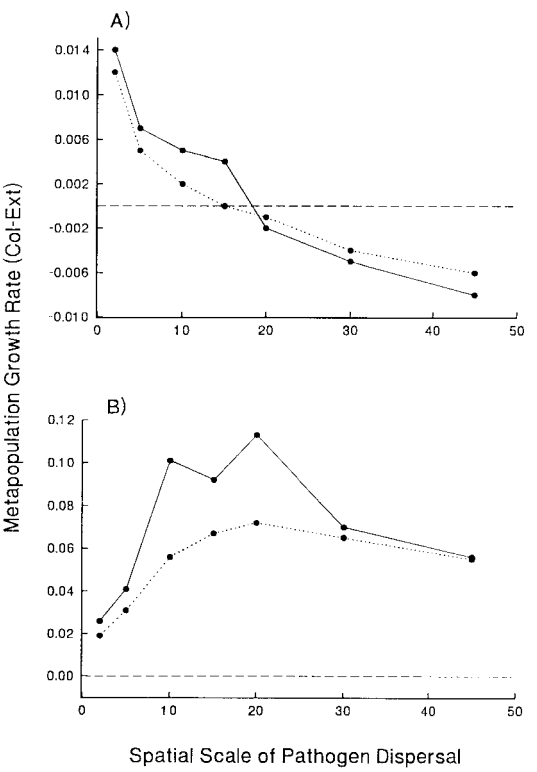

Fig. 3. Metapopulation growth rates (= colonization rates – extinction rates) as a function of the scale of pathogen dispersal. Solid lines are for host dispersal distance = 5; dotted lines are for host dispersal distance = 15. (A) Host growth rates, (B) pathogen growth rates. All data shown are for pathogen migration rate = 0.05. All other parameter values are the same as for Fig. 1.

Looking at colonization alone, rates were higher when host dispersal was at the larger scale (where the fraction of occupied sites was lower, and thus more sites were available for colonization); overall growth rates were less at the smaller scale of host dispersal because there was a proportionately greater decrease in extinction versus colonization rates.

In contrast, metapopulation growth rate for the pathogen was always positive, rising to a peak at intermediate scales of spore dispersal, before falling again (Fig. 3B). This pattern was much more pronounced when host dispersal distances were at the more local scale, and was generated by a marked increase in the pathogen colonization rate and a marginal decline in extinction rate for intermediate dispersal distances.

Distribution of disease severity

The scale of pathogen dispersal strongly affected the frequency distribution of disease severity levels (Fig. 4). The proportion of populations in the 0–5% severity category showed an initial sharp decrease, followed by a slow increase, as pathogen dispersal increased. This contrasted with the proportion of populations in the 95–100% severity category, where there was an initial sharp increase at low to intermediate scales of pathogen

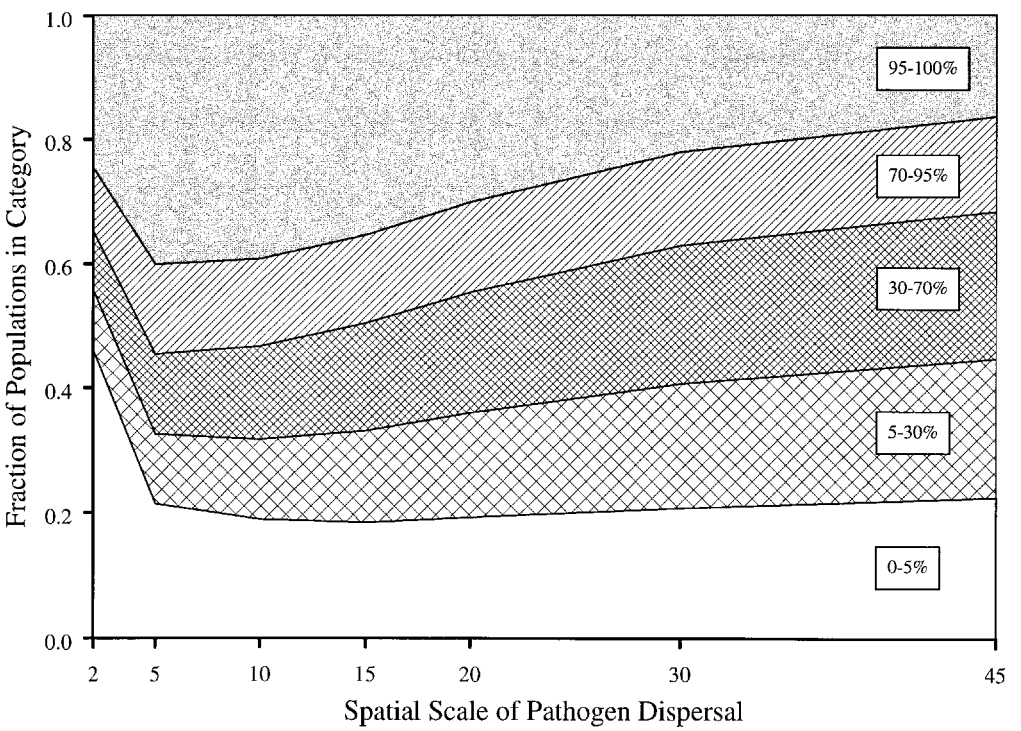

Fig. 4. Distribution of disease severity (defined as the average number of pustules per infected plant in diseased populations, where % is relative to the assumed maximum number of pustules per plant; see text) in relation to the spatial scale of pathogen dispersal. Data shown are for pathogen migration rate = 0.05 and host dispersal distance = 15 (essentially the same pattern was seen for all other combinations of pathogen migration rate and host dispersal distance). All other parameter values are the same as for Fig. 1.

dispersal, followed by an equally sharp decrease at higher scales of dispersal. The frequency of populations in the intermediate disease severity categories showed a consistent increase with the scale of pathogen dispersal. Overall, there was a relatively minor effect of pathogen migration rate or host dispersal distance, although at the higher host dispersal distance (= 15), there was generally a decrease in the frequency of populations with low or high disease severity, and an increase in intermediate levels of severity relative to the case when host dispersal was lower (= 5) (data not shown for this case).

Temporal dynamics and the scale of pathogen dispersal

Fluctuations in host and pathogen genotypes

There was considerable variability in the temporal dynamics of host and pathogen frequencies. However, the amplitude of fluctuations in genotype frequencies changed markedly with the spatial scale of pathogen dispersal (Fig. 5A). At extreme scales of pathogen dispersal

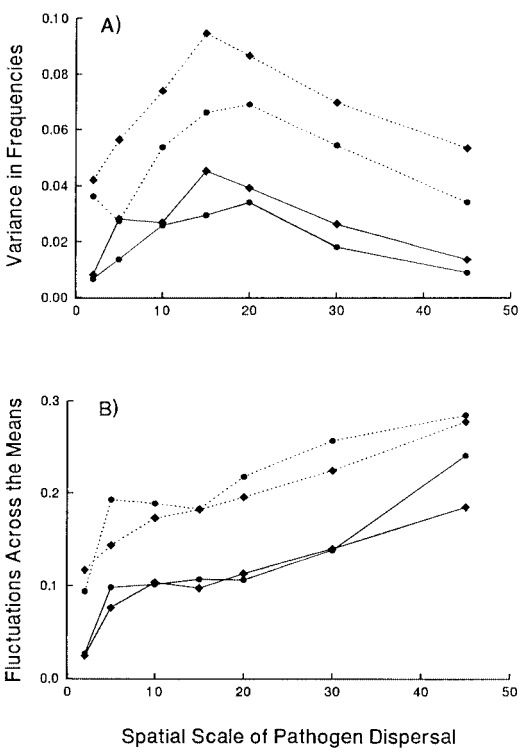

Fig. 5. Relationship between two measures of temporal dynamics with respect to host and pathogen frequencies (degree of oscillation and amplitude) and the scale of pathogen dispersal. (A) Variance in host and pathogen genotype frequencies; (B) number of times host and pathogen genotype frequencies fluctuated across the mean values [expressed as % of maximum possible out of 150 generations (= 74)]. Solid lines represent data for host frequencies and dotted lines represent pathogen frequencies [solid diamonds = low pathogen migration rate (0.05), solid circles = high pathogen migration rate (0.2)]. Other parameter values are the same as for Fig. 1.

where the metapopulation was behaving either as a collection of largely independent demes (2) or as a single large population with some substructuring (45), temporal variance in the frequencies was substantially less than that occurring for intermediate scales of dispersal. Not surprisingly, the amplitude of host fluctuations was always less than for the pathogen. Moreover, increasing the pathogen migration rate from 0.05 to 0.2 caused a substantial decrease in the amplitude (less so for the host). The average number of times that host or pathogen frequencies fluctuated across their mean values was positively related to the scale of pathogen dispersal (Fig. 5B). Regardless of pathogen migration rate, the number of fluctuations was always greater for the pathogen than for the host.

Correlation between host and pathogen frequencies

For both pathogen migration rates, the correlation between the frequency of the host and its associated pathogen genotype became increasingly positive as the scale of pathogen dispersal rose (Fig. 6, inset B). At the smallest dispersal distance, this involved a marked shift from a negative to a positive association (Fig. 6, inset A).

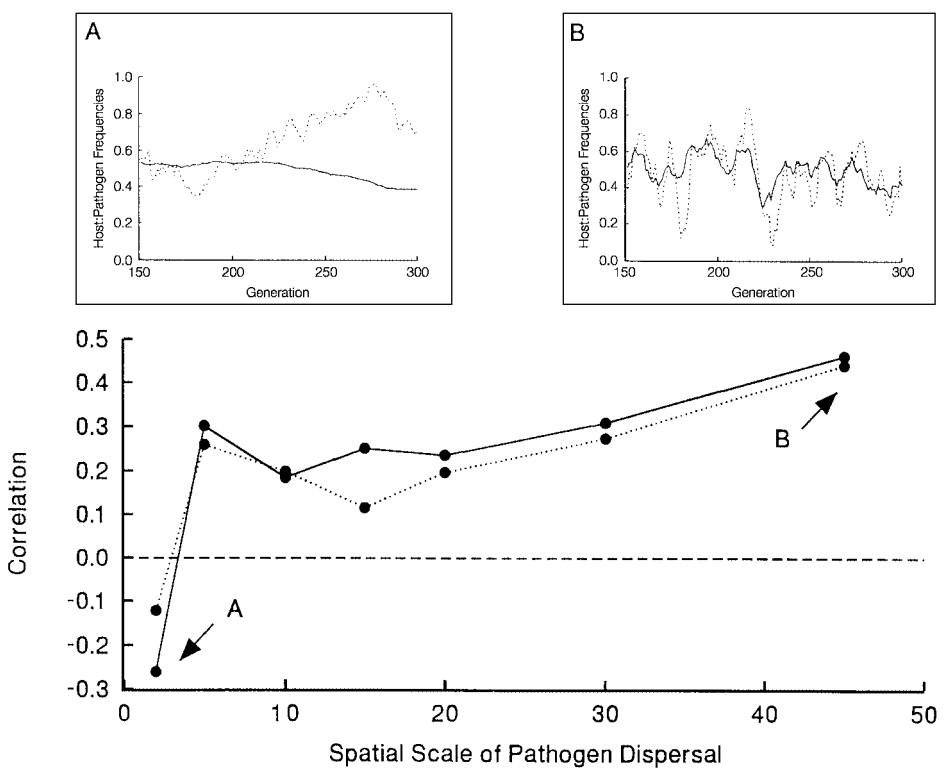

Fig. 6. Pearson product–moment correlation between associated host and pathogen frequencies (calculated across all sites in the simulation). Data shown are for host dispersal distance = 15; solid lines = low pathogen migration rate (0.05); dotted lines = high pathogen migration rate (0.2). The insets show, for representative runs, the changes in host and pathogen frequencies across time [A = local pathogen dispersal (2), B = large-scale pathogen dispersal (45)]. Other parameter values are the same as for Fig. 1.

The temporal variation in the fraction of populations with disease present showed a non-linear response to changes in the spatial scale of spore dispersal, rising from a minimum at the lowest scale (2) to a peak at intermediate dispersal distances, before declining at the largest scales of dispersal (the data presented in Fig. 7 are variances; however, the coefficient of variation showed the same pattern). This reflects a shift from an endemic pattern of very little fluctuation in the proportion of diseased populations (Fig. 7, inset A) to chaotic fluctuations (Fig. 7, inset B) and, finally, to increasingly regular cyclical behaviour (Fig. 7, inset C).

Overall, these results underline the qualitative changes in the dynamic behaviour of the metapopulation as the scale of pathogen dispersal increased. Thus, at very low scales of dispersal, the dynamics could be characterized by relatively low amplitude and oscillatory behaviour. At intermediate scales of dispersal, the amplitude was at a peak, with increasing oscillatory behaviour. At the largest scale of pathogen dispersal, oscillatory behaviour was greatest, while amplitude again decreased to somewhat lower levels. Similar patterns were seen with respect to fluctuations in the fraction of diseased populations across the metapopulation.

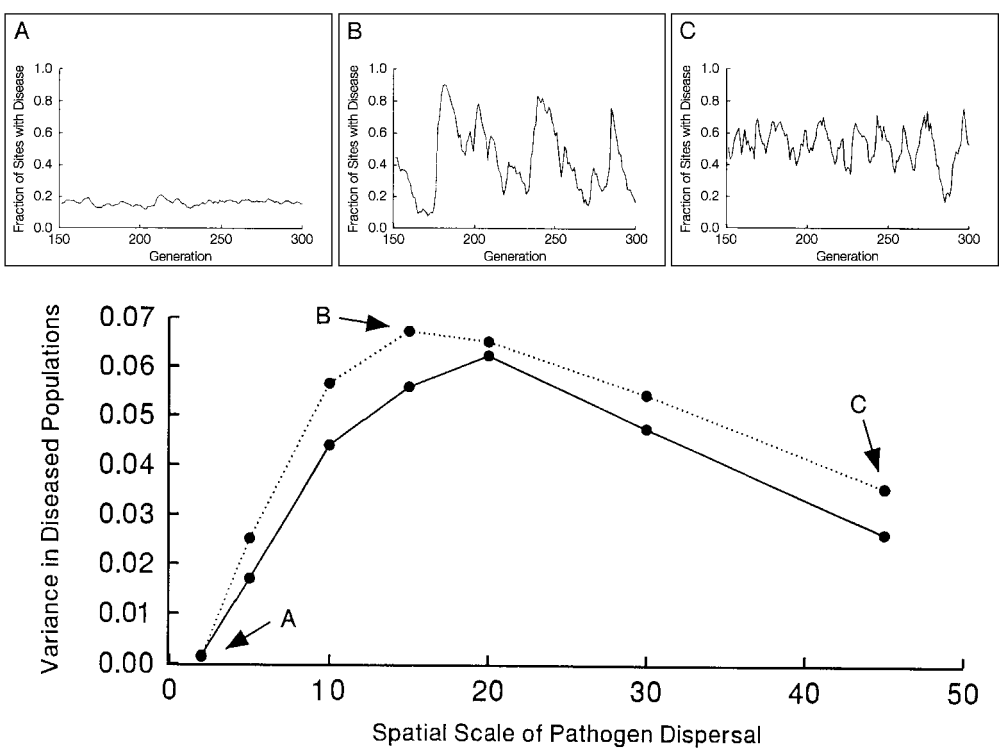

Fig. 7. Relationship between temporal fluctuations in disease levels and the scale of pathogen dispersal. Data shown are for host dispersal distance = 15; solid lines = low pathogen migration rate (0.05); and dotted lines = high pathogen migration rate (0.2). The insets show, for representative runs, the temporal changes in the fraction of occupied sites that are diseased [A = local pathogen dispersal (2), B = intermediate pathogen dispersal (15), C = large-scale pathogen dispersal (45)]. Other parameters are the same as for Fig. 1.

With respect to spatial structure, plots of Moran's *I* showed strong positive correlations at scales at or less than 10 population units for both host frequency and disease prevalence. However, in general, there were no obvious effects of either the scale of pathogen dispersal or migration rate on patch size.

DISCUSSION

It is now widely recognized that spatial structure can substantially alter the dynamics of a system from expectations based on models of single populations (Nee *et al.*, 1997). The addition of spatial structure may result in qualitative changes in the conditions for co-existence, such that even when within-population persistence cannot occur, persistence at larger spatial scales is possible as a result of a balance between local colonization and extinction. This scenario is a reasonable one for many host–pathogen systems which are often typified by 'boom and bust' cycles (Burdon, 1993) that clearly run counter to the recent argument that 'empirical evidence casts doubt' on the importance of colonization/extinction dynamics (Hastings and Harrison, 1994; Harrison and Hastings, 1996).

Plant pathogenic fungi and their hosts show an enormous diversity of life-history strategies (e.g. patterns of dispersal). The combined effect of variation in both host and pathogen characters is likely to lead to interactions showing a range of quite distinct spatial scales (Thrall and Burdon, 1997). At one extreme (e.g. soil pathogens), spatial structure may be best represented by many small relatively unconnected populations, while at the other extreme (e.g. aerially dispersed rusts), spatial structure may resemble much more closely a large global population with some degree of substructuring. In the present paper, we have explored the consequences of variation in spatial structure for disease persistence, and for the nature of both spatial and temporal dynamics. Overall, our results show that the scale of pathogen dispersal can have significant impacts on the type of dynamics (endemic *vs* epidemic) as well as the likelihood of disease persistence. More generally, this suggests that the evolution of disease characteristics (e.g. severity of impacts on host fitness) will also, at least in part, be determined by the scale of the spatial interaction between host and pathogen (Frank, 1997).

Disease persistence and patterns of incidence

In this study, disease persistence was strongly affected by both migration rate and the spatial scale of host and pathogen dispersal, with persistence being highest at lower scales of dispersal and low rates of pathogen migration. Similarly, Gandon *et al.* (1996) found significant variation in disease persistence, although their model focused on the effects of pathogen migration rate, rather than the spatial scale of dispersal. A number of other theoretical studies have also shown that systems of interconnected and locally unstable patches are most likely to persist with intermediate rates of migration: that is, if local patches are completely isolated, then local extinction occurs; if completely connected, then metapopulation extinction occurs due to synchronous dynamics (with respect to predator–prey or host–parasitoid models, see Caswell, 1978; Sabelis *et al.*, 1991; Taylor, 1991; Comins *et al.*, 1992). It should be noted that metapopulation persistence will also be heavily dependent on the size of the spatial arena (which determines the availability of sites for colonization), with larger arenas leading to increased persistence (Nee *et al.*, 1997).

One explanation for the dependence of disease persistence on dispersal scale is that pathogen persistence is likely to be enhanced when spore dispersal is at similar or smaller spatial scales than host dispersal. Under these conditions, disease spreads less rapidly in neighbouring populations than when scales of pathogen dispersal are much greater than that of the host. Roughly speaking, disease persistence will be reduced at higher scales of dispersal to the extent that spread of disease into neighbouring populations is higher than the rate at which the host colonizes new sites. This may be why a highly virulent pathogen cannot persist if the rate at which neighbouring sites become diseased is high (e.g. highly virulent soil-borne pathogens must have a long-distance aerial dispersal mechanism, a wide host range and/or free-living stages such as being saprophytic). Disease persistence is further depressed as the migration rate of the pathogen increases for any particular scale of dispersal. This is illustrated by comparing changes in the fraction of occupied sites (Fig. 2A) with changes in the pathogen growth rate across the metapopulation as a whole (highest at intermediate dispersal due to high colonization/extinction rates; Fig. 3B), and the nature of the ensuing dynamics (most chaotic at intermediate scales of dispersal; Fig. 7). Together, these results all imply that pathogen persistence is likely to be lowest when its spread in the metapopulation is most rapid. The product of these factors, resulting from shifts in the scale of pathogen dispersal, will ultimately determine 'opportunities' for pathogen spread and persistence in the metapopulation.

The data on metapopulation growth rates show that host growth declines steadily, becoming negative as pathogen dispersal becomes more global. In contrast, pathogen metapopulation growth rates are always positive, but when the migration rate is low (= 0.05), show a much larger increase (relative to when the migration rate is 0.2) at intermediate scales of dispersal (Fig. 3). This suggests that pathogen spread at the metapopulation level is greatest for the intermediate range of dispersal (corresponding to the region where pathogen persistence is lowest). It is also at these intermediate scales of dispersal, where the amplitude of fluctuations in both host and pathogen genotype frequencies, and the fraction of diseased populations, is greatest (Fig. 2). Increasing fluctuation in these parameters leads to increasing probability of global extinction as a consequence of stochastic effects. Frank (1993) showed that the stability of within-population host and pathogen dynamics were similarly dependent on the rate of pathogen increase, with population sizes fluctuating more at higher pathogen growth rates.

The apparently anomalous situation whereby host growth rates are negative (implying extinction of the metapopulation as a whole) is probably due to the fact that, in the simulation, we measured 'apparent' rather than 'actual' colonization and extinction rates because the former are parameters that can actually be measured in the field. Actual rates, on the other hand, include highly ephemeral and generally undetectable events where host or pathogen extinction is followed by immediate recolonization within the course of a transition between generations. Evidence that the simulation was not on the way to global extinction is that, for any run that persisted to 300 generations, the fraction of occupied sites varied only slightly around the mean value (there were no cases observed where the pathogen caused complete extinction of the host).

Population and metapopulation dynamics

Simulation of a deterministic model of a single population (i.e. equations 7–9 with no migration) showed that, for the range of parameter values investigated, two dynamical

outcomes were possible. Under some conditions, host and pathogen showed oscillatory convergence to a stable equilibrium, but with the host near the population carrying capacity and the disease only present at extremely low levels between epidemic phases (as is typical of non-systemic rusts). In other cases, the pathogen was lost from the population and the host converged to the disease-free carrying capacity. Overall, these results indicate that disease persistence in single populations would be very unlikely in systems where there is significant within-season disease spread, and infection causes high mortality. Persistence is most likely only possible in a metapopulation, where there is significant pathogen movement among local populations.

As expected, when dispersal is extremely local, the simulation behaves as a collection of many small independent populations (with disease dynamics being more endemic when averaged across the metapopulation); when the scale of pathogen dispersal is nearly global, the simulation behaves as a single large population. Interestingly, it is at the intermediate scales of pathogen dispersal that dynamics are the most chaotic with respect to disease prevalence and presence/absence. This unpredictable appearance and disappearance of disease in local populations suggests that it is at these scales that colonization/extinction dynamics are probably most important in determining the overall persistence of disease in the system, as well as the underlying genetic structure of resistance and virulence (Frank, 1993, 1997).

Overall, both the degree to which dynamics were oscillatory (measured in terms of fluctuations across mean values) and the amplitude of such oscillations (measured as variance across generations) decreased as the pathogen dispersal distance became increasingly localized (Fig. 5). This is to be expected, since within-population dynamics become increasingly asynchronous as the scale of dispersal decreases. In these circumstances, individual population fluctuations will cancel each other out, leading to lower fluctuations in global frequencies. In contrast, when the scale of dispersal was very large (and therefore the metapopulation was behaving essentially as a single large population), within-population dynamics were most synchronous and therefore the degree to which dynamics were oscillatory was also greatest. Our data also show that, from a metapopulation perspective, dynamics are endemic when pathogen dispersal is at very local scales, but epidemic when at much larger scales (at intermediate scales, disease can remain low over extended periods of time, but then increase rapidly in a few generations; see Fig. 7). However, even when disease is behaving endemically at the metapopulation level, full-scale epidemics may still occur within individual populations.

It was particularly interesting that, at very local scales of pathogen dispersal (less than that of the host), there was a negative correlation between the frequencies of hosts and their associated pathogens (Fig. 6). In contrast, a spatially explicit model of anther-smut disease in *Silene alba* showed a positive correlation between the susceptible host type and disease prevalence; empirical support for this result was subsequently obtained from field experiments (Thrall and Antonovics, 1995). However, in that study, disease dynamics were only examined at quite local spatial scales (similar to the most local scales of dispersal examined in the present study). Among-population disease movement in the *Silene–Ustilago* system is likely to be over much shorter distances than in aerially dispersed rusts, as it is vector-transmitted by insect pollinators (Antonovics *et al.*, 1994; Thrall and Antonovics, 1995). Overall, whether one would expect to find positive or negative correlations between susceptible hosts and their pathogens is likely to depend on rates of disease spread across the metapopulation, population turnover and the strength of selection against susceptible host

types; these will all be influenced by the spatial scale of pathogen dispersal relative to that of the host.

Evolutionary implications

Burdon *et al.* (1996) proposed that the evolution and maintenance of gene-for-gene systems was likely to be favoured in associations where host phenology and life-history patterns would promote pathogen dynamics typified by relatively frequent population crashes and local extinctions. They further argued that stochasticity in encounter rates between a particular host and the pathogens to which it was susceptible would enhance the advantage of retaining 'unnecessary' genes for resistance.

More recently, Thrall and Burdon (1997) suggested that the relative scales at which hosts and pathogens interact may have similar consequences for the evolution of resistance and virulence structure by influencing the frequency of encounter between a given host genotype and the pathogen genotypes to which it is susceptible. For example, the continuum in the relative spatial scale of host and pathogen dispersal (with aerially dispersed rusts such as in the *Linum–Melampsora* system at one extreme, and soil-borne pathogens such as *Rhizoctonia* at the other) also parallels a continuum in the degree of predictability of encounter between particular host and pathogen genotypes. As the predictability and frequency of encounter between host and pathogen increases with declining spatial and temporal variability, the relative proportion of the host's life-cycle during which disease is absent decreases, and conditions are approached in which race specific resistance may confer little benefit. In these circumstances, selection may tend to favour resistance that is based on many genes (qualitative resistance) rather than on single genes (gene-for-gene interactions; quantitative resistance). Although empirical data on the incidence and importance of qualitative versus quantitative resistance in natural systems are limited (Burdon *et al.*, 1996), those studies that exist show a strong bias in the occurrence of gene-for-gene interactions among host–pathogen associations characterized by broader spatial scales of pathogen dispersal.

The relative scale of dispersal of host and pathogen in the interaction metapopulation may also impose constraints on the overall aggressiveness of the pathogen. Thus, for highly specialized pathogens which rely entirely on single host species for survival, as the spatial scale of dispersal decreases relative to that of the host, there is likely to be a corresponding decrease in the maximum selection pressure the pathogen can exert without leading to its own demise. For many of these interactions, increasingly endemic (as opposed to epidemic) population dynamics may be most common; the degree to which this expectation is met will further depend on whether the pathogen is systemic (one to a few pathogen cycles per host generation) or localized on the plant (multiple pathogen cycles per host generation). Interestingly, a very wide range of pathogens that would normally have characteristics associated with this restricted distribution category have avoided this bottleneck through various combinations of multiple host ranges and/or the ability to grow and survive as saprophytes. For hosts of these pathogens, escape in time and space is frequently not possible and quantitatively based resistance is likely to be more effective than qualitatively based gene-for-gene mechanisms.

Overall, a consideration of the types of spatial interaction that exist in natural plant–pathogen systems will shed considerable light on: (1) the evolution of pathogen life-history features [e.g. severity and type of effects on the host (fecundity *vs* mortality), the importance

of free-living stages]; (2) the types of dynamics that are likely to occur (epidemic *vs* endemic dynamics); and (3) perhaps most importantly, the consideration of spatial structure and its influence on evolution in host–pathogen systems may provide some degree of prediction with respect to the types of situations in which complex resistance/virulence structures (i.e. gene-for-gene) are most likely to occur.

ACKNOWLEDGEMENTS

The manuscript was improved by the suggestions and comments of A. Young, A.H.D. Brown and R.H. Groves. We also thank L.A. Real and an anonymous reviewer for their careful consideration of the final version of the paper.

REFERENCES

Alexander, H.M. and Antonovics, J. 1988. Disease spread and population dynamics of anther-smut infection of *Silene alba* caused by the fungus *Ustilago violacea*. *J. Ecol.*, **76**: 91–104.

Alexander, H.M., Thrall, P.H., Antonovics, J., Jarosz, A.M. and Oudemans, P.V. 1996. Population dynamics and genetics of plant disease: A case study of anther-smut disease. *Ecology*, **77**: 990–996.

Antonovics, J., Thrall, P.H., Jarosz, A.M. and Stratton, D. 1994. Ecological genetics of meta-populations: The *Silene–Ustilago* plant–pathogen system. In *Ecological Genetics* (L. Real, ed.), pp. 146–170. Princeton, NJ: Princeton University Press.

Antonovics, J., Thrall, P.H. and Jarosz, A.M. 1997. Genetics and the spatial ecology of species interactions: The *Silene–Ustilago* system. In *Spatial Ecology: The Role of Space in Population Dynamics and Interspecific Interactions* (D. Tilman and P. Kareiva, eds), pp. 158–180. Princeton, NJ: Princeton University Press.

Burdon, J.J. 1993. The structure of pathogen populations in natural plant communities. *Ann. Rev. Phytopathol.*, **31**: 305–323.

Burdon, J.J. and Elmqvist, T. 1996. Selective sieves in the epidemiology of *Melampsora lini*. *Plant Pathol.*, **45**: 933–943.

Burdon, J.J. and Jarosz, A.M. 1991. Host–pathogen interactions in natural populations of *Linum marginale* and *Melampsora lini*: I. Patterns of resistance and racial variation in a large host population. *Evolution*, **45**: 205–217.

Burdon, J.J. and Jarosz, A.M. 1992. Temporal variation in the racial structure of flax rust (*Melampsora lini*) populations growing on natural stands of wild flax (*Linum marginale*): Local versus metapopulation dynamics. *Plant Pathol.*, **41**: 165–179.

Burdon, J.J. and Thompson, J.N. 1995. Changed patterns of resistance in a population of *Linum marginale* attacked by the rust pathogen *Melampsora lini*. *J. Ecol.*, **83**: 199–206.

Burdon, J.J., Ericson, L. and Muller, W.J. 1995. Temporal and spatial changes in a metapopulation of the rust pathogen *Triphragmium ulmariae* and its host, *Filipendula ulmaria*. *J. Ecol.*, **83**: 979–989.

Burdon, J.J., Wennstrom, A., Elmqvist, T. and Kirby, G.C. 1996. The role of race specific resistance in natural plant populations. *Oikos*, **76**: 411–416.

Carlsson, U., Elmqvist, T., Wennstrom, A. and Ericson, L. 1990. Infection by pathogens and population age of host plants. *J. Ecol.*, **78**: 1094–1105.

Caswell, H. 1978. Predator-mediated coexistence: A non-equilibrium model. *Am. Nat.*, **112**: 127–154.

Comins, H.N., Hassell, M.P. and May, R.M. 1992. The spatial dynamics of host–parasitoid systems. *J. Anim. Ecol.*, **61**: 735–748.

Frank, S.A. 1991. Ecological and genetic models of host–pathogen coevolution. *Heredity*, **67**: 73–83.

Frank, S.A. 1993. Coevolutionary genetics of plants and pathogens. *Evol. Ecol.*, **7**: 45–75.

Frank, S.A. 1997. Spatial processes in host–parasite genetics. In *Metapopulation Biology: Ecology, Genetics and Evolution* (I. Hanski and M.E. Gilpin, eds), pp. 325–352. San Diego, CA: Academic Press.

Gandon, S., Capowiez, Y., Dubois, Y., Michalakis, Y. and Olivieri, I. 1996. Local adaptation and gene-for-gene coevolution in a metapopulation model. *Proc. Roy. Soc. Lond. B*, **263**: 1003–1009.

Gilpin, M.E. 1975. *Group Selection in Predator–Prey Communities*. Princeton, NJ: Princeton University Press.

Hanski, I. and Gilpin, M.E., eds. 1997. *Metapopulation Dynamics: Ecology, Genetics and Evolution*. New York: Academic Press.

Harrison, S. and Hastings, A. 1996. Genetic and evolutionary consequences of metapopulation structure. *Trends Ecol. Evol.*, **11**: 180–183.

Hastings, A. and Harrison, S. 1994. Metapopulation dynamics and genetics. *Ann. Rev. Ecol. Syst.*, **25**: 167–188.

Jarosz, A.M. and Burdon, J.J. 1991. Host–pathogen interactions in natural populations of *Linum marginale* and *Melampsora lini*: II. Local and regional variation in patterns of resistance and racial structure. *Evolution*, **45**: 1618–1627.

Jarosz, A.M. and Burdon, J.J. 1992. Host–pathogen interactions in natural populations of *Linum marginale* and *Melampsora lini*: III. Influence of pathogen epidemics on host survivorship and flower production. *Oecologia*, **89**: 53–61.

Leonard, K.J. 1969. Selection in heterogeneous populations of *Puccinia graminis* f. sp. *avenae*. *Phytopathology*, **84**: 70–77.

Levins, R. 1969. Some demographic and genetic consequences of environmental heterogeneity for biological control. *Bull. Entomol. Soc. Am.*, **15**: 237–240.

Levins, R. 1970. Extinction. In *Some Mathematical Problems in Biology* (M. Gerstenhaber, ed.), pp. 77–107. Providence, RI: American Mathematical Society.

Martz, H.F. and Waller, R.A. 1982. *Bayesian Reliability Analysis*. New York: John Wiley.

McCauley, D.E. 1994. Contrasting the distribution of chloroplast DNA and allozyme polymorphism among local populations of *Silene alba*: Implications for studies of gene flow in plants. *Proc. Nat. Acad. Sci. USA*, **91**: 8127–8131.

McCauley, D.E., Raveill, J. and Antonovics, J. 1995. Local founding events as determinants of genetic structure in a plant metapopulation. *Heredity*, **75**: 630–636.

Nee, S., May, R.M. and Hassell, M.P. 1997. Two-species metapopulation models. In *Metapopulation Biology: Ecology, Genetics and Evolution* (I. Hanski and M.E. Gilpin, eds), pp. 123–147. San Diego, CA: Academic Press.

Sabelis, M.W., Diekmann, O. and Jansen, V.A.A. 1991. Metapopulation persistence despite local extinction: Predator–prey patch models of the Lotka-Volterra type. *Biol. J. Linn. Soc.*, **42**: 267–283.

Taylor, A.D. 1991. Studying metapopulation effects in predator–prey systems. *Biol. J. Linn. Soc.*, **42**: 305–323.

Thrall, P.H. and Antonovics, J. 1995. Theoretical and empirical studies of metapopulations: Population and genetic dynamics of the *Silene–Ustilago* system. *Can. J. Bot.*, **73**(suppl. 1): S1249–S1258.

Thrall, P.H. and Burdon, J.J. 1997. Host–pathogen dynamics in a metapopulation context: The ecological and evolutionary consequences of being spatial. *J. Ecol.*, **85**: 743–753.

Thrall, P.H. and Jarosz, A.M. 1994a. Host–pathogen dynamics in experimental populations of *Silene alba* and *Ustilago violacea* I. Ecological and genetic determinants of disease spread. *J. Ecol.*, **82**: 549–559.

Thrall, P.H. and Jarosz, A.M. 1994b. Host–pathogen dynamics in experimental populations of *Silene alba* and *Ustilago violacea* II. Experimental tests of theoretical models. *J. Ecol.*, **82**: 561–570.

Thrall, P.H., Biere, A. and Antonovics, J. 1993. Plant life-history and disease susceptibility: The occurrence of *Ustilago violacea* on different species within the Caryophyllaceae. *J. Ecol.*, **81**: 489–498.

Thrall, P.H., Richards, C.M., McCauley, D.E. and Antonovics, J. 1998. Metapopulation collapse: The consequences of limited gene-flow in spatially structured populations. In *Modelling Spatio-temporal Dynamics in Ecology* (J. Bascompte and R.V. Sole, eds), pp. 83–104. Berlin: Springer-Verlag.

Tilman, D. and Kareiva, P., eds. 1997. *Spatial Ecology: The Role of Space in Population Dynamics and Interspecific Interactions*. Princeton, NJ: Princeton University Press.

APPENDIX: DEFINITIONS OF MODEL PARAMETERS AND SYMBOLS

X population size of healthy host plants
Y population size of infected plants
P pathogen population size (total number of pustules within a host population)
N total host population size ($= X + Y$)
b_0 maximum per-capita plant reproductive rate
ζ constant that determines the strength of density-dependent host growth
β phenomenological disease transmission coefficient
k number of infection cycles per host growing season
ε rate of recovery for infected hosts
γ rate of pustule production per existing pustule
μ_X mortality rate for healthy plants
μ_Y mortality rate for infected plants, dependent on level of disease severity (the number of pustules per plant; see equation 11)
μ_0 maximum mortality rate for infected plants
λ determines rate at which mortality increases with disease severity
μ_{PS} within-season mortality rate for pustules
μ_{PW} over-winter mortality rate for pustules